Int. J. Solids Structures Vol. 23, No. 8, pp. 1123–1132, 1987
Printed in Great Britain.

0020-7683/87 $3.00+.00

NON-LINEAR FREE VIBRATION AND POSTBUCKLING OF SYMMETRICALLY LAMINATED ORTHOTROPIC IMPERFECT SHALLOW CYLINDRICAL PANELS WITH TWO ADJACENT EDGES SIMPLY SUPPORTED AND THE OTHER EDGES CLAMPED

CHUEN-YUAN CHIA
Department of Civil Engineering, University of Calgary, Calgary, Alberta, Canada T2N 1N4

(*Received* 10 *June* 1986; *in revised form* 3 *September* 1986)

Abstract—A unified approximate solution to the Marguerre-type equations for the titled problem is formulated by the use of the Galerkin procedure. The corresponding flat-plate problem is treated as a special case. Numerical results for fundamental non-linear free vibration and postbuckling behavior of isotropic, orthotropic and symmetrically laminated cross-ply shallow cylindrical panels are presented for various curvatures, in-plane forces, geometrically initial imperfections, and geometries of laminations. Present results are compared with available data.

NOTATION

$A_{22}, \bar{A}_{22}$ $a_i, b_i, \bar{D}_{11}$	constants of a panel, see around eqns (3)
a, b	length and arc width of a panel
C_{pq}, F_{pq}	Fourier constants, see eqn (8)
$c, \bar{c}$	normalized constants, see eqns (9)
D	flexural rigidity of an isotropic plate
E_L, E_T, G_{LT}	principal and shear moduli of an orthotropic layer or plate
F	non-dimensional stress function, see eqns (3)
f	function of non-dimensional time
h	thickness of a panel
J	constant, see eqn (20)
K_R	non-dimensional curvature, see eqns (3)
K_i^{km}, L_j^{ln}	definite integrals, see Appendix
N_{cr}, n_{cr}	dimensional and non-dimensional critical buckling loads per unit length in the direction of straight edges, see eqn (25)
n_x, n_y, n_z	dimensional and non-dimensional in-plane edge forces per unit length, respectively, see eqns (5)
R	radius of a cylindrical panel
r	ratio of in-plane edge forces
t	time
$W, \bar{W}$	non-dimensional deflection and initial deflection, see eqns (3)
$\bar{W}_0$	amplitude of non-dimensional initial deflection
$W_{mn}, \bar{W}_{mn}$	coefficients in eqns (6) and (7), respectively
$w, w_{max}, \bar{w}$	deflection, maximum deflection and initial deflection, respectively
X_i, Y_j	orthogonal functions, see eqns (9)
x, y, z	rectangular Cartesian coordinates
β_j, γ_j	coefficients, see eqns (10)
$\delta_1, \delta_2, \delta_3$ $\varepsilon_1, \varepsilon_2$	coefficients, see eqns (15)–(19)
ζ, η	non-dimensional coordinates, see eqns (3)
ζ_1, η_1	coordinates of the location at which w_{max} occurs
λ	ratio of length to arc width of a panel
ρ	panel mass per unit area
τ	non-dimensional time, see eqns (3)
ψ	stress function
ϕ_m, ψ_n	orthogonal functions, see eqns (9)
$\omega, \omega^{(0)}$	non-linear and linear frequencies, respectively
ω_0	linear frequency parameter, see eqn (21).

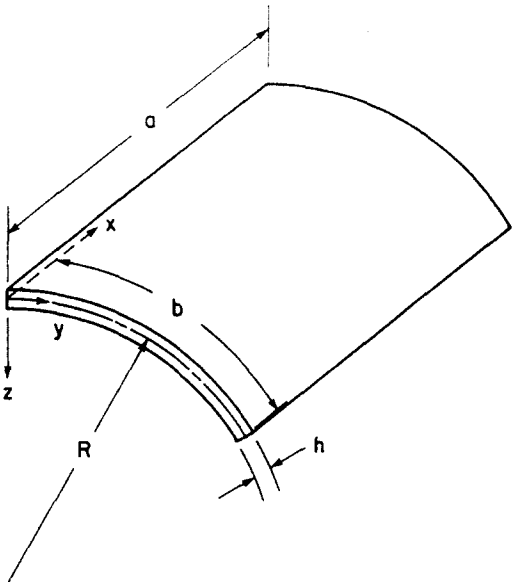

Fig. 1. Geometry and coordinate system of a shallow cylindrical panel.

INTRODUCTION

Non-linear vibration and postbuckling of elastic plates have received considerable attention in recent years. A comprehensive review of the literature may be found in Ref. [1] or elsewhere. Most of the existing solutions are restricted to uniform boundary conditions. In the case of rectangular plates with mixed boundary conditions several non-linear solutions in the sense of von Kármán are available for isotropic[2], orthotropic[3, 4], anisotropic[5] and laminated composite[6, 7] materials. These results, however, are all restricted to boundary conditions symmetrical with respect to the centre lines of a rectangular plate. Non-linear solutions for rectangular plates with unsymmetric boundary conditions cannot be found in the literature.

This paper deals with non-linear free flexural vibration of a symmetrically laminated shallow cylindrical panel of geometrically initial imperfections with two adjacent edges clamped and the other edges simply supported. The panel is subjected to in-plane tensions along its four edges but not the tangential boundary forces. The dynamic Marguerre-type equations adopted for the panel are expressed in terms of the deflection and the stress function. A single-mode analysis is carried out and the stress function is represented by the product of a time function and generalized Fourier series in terms of spacial coordinates. The Galerkin procedure furnishes an equation for the time function which is solved by the use of the perturbation method. The postbuckling behaviour of the panel is treated as a special case.

GOVERNING EQUATIONS

Consider a shallow cylindrical panel of midsurface radius R, thickness h, length a in the x-direction and arc width b in the y-direction as shown in Fig. 1. The midsurface of the undeformed panel contains the x- and y-axes. The panel is assumed to consist of n layers of orthotropic sheets perfectly bonded together. Each layer has arbitrary thickness, elastic properties, and orientation of orthotropic axes with respect to the plate axes. However, the layers are so arranged that a midsurface symmetry exists. That is, for each layer above the midsurface, there is a corresponding layer identical in thickness, elastic properties, and orientation located at the same distance below the midsurface. Including the initial curvature of the panel in eqns (2–167) of Ref. [1] and following the derivation for eqns (1–153) and (1–154) of the reference, the dynamic Marguerre-type equations of the panel are obtained.

Ignoring the in-plane and rotary inertia effects, these basic equations governing the non-linear free flexural vibration of the panel of geometrically initial imperfections in the sense of von Kármán may be expressed in the following non-dimensional form:

$$W_{,\zeta\zeta\zeta\zeta}+a_1\lambda W_{,\zeta\zeta\zeta\eta}+2a_2\lambda^2 W_{,\zeta\zeta\eta\eta}+a_3\lambda^3 W_{,\zeta\eta\eta\eta}+a_4\lambda^4 W_{,\eta\eta\eta\eta}$$
$$+\lambda^4 W_{,\tau\tau}/\bar{D}_{11}-(\lambda^2/\bar{D}_{11})[F_{,\zeta\zeta}(K_R+W_{,\eta\eta}+\bar{W}_{,\eta\eta}$$
$$+F_{,\eta\eta}(W_{,\zeta\zeta}+\bar{W}_{,\zeta\zeta})-2F_{,\zeta\eta}(W_{,\zeta\eta}+\bar{W}_{,\zeta\eta})]=0 \quad (1)$$

$$F_{,\zeta\zeta\zeta\zeta}-b_1\lambda F_{,\zeta\zeta\zeta\eta}+2b_2\lambda^2 F_{,\zeta\zeta\eta\eta}-b_3\lambda^3 F_{,\zeta\eta\eta\eta}+b_4\lambda^4 F_{,\eta\eta\eta\eta}$$
$$=(\lambda^2/\bar{A}_{22})[W_{,\zeta\eta}^2-W_{,\zeta\zeta}(K_R+\bar{W}_{,\eta\eta})-W_{,\eta\eta}(W_{,\zeta\zeta}+\bar{W}_{,\zeta\zeta})+2W_{,\zeta\eta}\bar{W}_{,\zeta\eta}] \quad (2)$$

in which the subscripts preceded by a comma denote differentiation with respect to the corresponding coordinates and coefficients a_i, b_i, $\bar{D}_{11}$ and $\bar{A}_{22}$ are constants of the panel given by the corresponding coefficients in eqns (5–201) and (5–202) of Ref. [1] and in which

$$\zeta=\frac{x}{a},\qquad \eta=\frac{y}{b},\qquad \tau=\frac{t}{b^2}\sqrt{(A_{22}h^2/\rho)},\qquad W=\frac{w}{h}$$
$$\bar{W}=\frac{\bar{w}}{h},\qquad F=\frac{\psi}{A_{22}h^2},\qquad \lambda=\frac{a}{b},\qquad K_R=\frac{b^2}{Rh}. \quad (3)$$

In these expressions w is the deflection, $\bar{w}$ the initial deflection, ψ the stress function, t the time, ρ the panel mass per unit area, and A_{22} the membrane rigidity of the panel in the y-direction.

Two adjacent edges of the plate at $\zeta = 0$ and at $\eta = 0$ are assumed to be clamped and the other edges to be simply supported. The panel is subjected to biaxial edge forces per unit length, n_x in the x-direction and n_y in the y-direction, but not the tangential boundary forces. These boundary conditions for a symmetrically laminated cross-ply panel may be written in the non-dimensional form as

$$W=0,\qquad F_{,\eta\eta}=n_\zeta,\qquad F_{,\zeta\eta}=0 \quad \text{at} \quad \zeta=0,1$$
$$W=0,\qquad F_{,\eta\eta}=\lambda^2 r n_\zeta,\qquad F_{,\zeta\eta}=0 \quad \text{at} \quad \eta=0,1 \quad (4)$$
$$W_{,\zeta}|_{\zeta=0}=0,\qquad W_{,\zeta\zeta}|_{\zeta=1}=0,\qquad W_{,\eta}|_{\eta=0}=0,\qquad W_{,\eta\eta}|_{\eta=1}=0$$

where

$$n_\zeta=n_x b^2/A_{22}h^2,\qquad r=n_y/n_x. \quad (5)$$

The system of eqns (1) and (2) are thus to be solved in conjunction with boundary conditions (4).

ANALYSIS

A single-mode analysis is carried out in this work. As usual a solution of eqns (1) and (2) is sought in the separable form

$$W=cf(\tau)\sum_{m,n=1,3}^{M}\sum^{N} W_{mn}\phi_m(\zeta)\psi_n(\eta) \quad (6)$$

$$\bar{W}=\bar{c}\bar{W}_0\sum_{m,n=1,3}^{M}\sum^{N} \bar{W}_{mn}\phi_m(\zeta)\psi_n(\eta) \quad (7)$$

$$F = \tfrac{1}{2}n_\zeta(\eta^2+\lambda^2 r\zeta^2)+f(\tau)\sum_{p,q=1}^{\infty}\sum C_{pq}X_p(\zeta)Y_q(\eta)+f^2(\tau)\sum_{p,q=1}^{\infty}\sum F_{pq}X_p(\zeta)Y_q(\eta). \tag{8}$$

In these equations f is a function of τ to be determined and ϕ_m, ψ_n, X_p, Y_q, c and $\bar{c}$ are defined by

$$\begin{aligned}
\phi_m &= \cos(m\pi\zeta/2)-\cos(3m\pi\zeta/2)\\
\psi_n &= \cos(n\pi\eta/2)-\cos(3n\pi\eta/2)\\
X_p &= \cosh\beta_p\zeta-\cos\beta_p\zeta-\gamma_p(\sinh\beta_p\zeta-\sin\beta_p\zeta)\\
Y_q &= \cosh\beta_q\eta-\cos\beta_q\eta-\gamma_q(\sinh\beta_q\eta-\sin\beta_q\eta)\\
c &= \left[\sum_{m,n=1,3}\sum W_{mn}\phi_m(\zeta_1)\psi_n(\eta_1)\right]^{-1}
\end{aligned} \tag{9}$$

where ζ_1 and η_1 are coordinates of the location at which the maximum deflection $w_{\max}$ occurs and $\bar{c}$ is obtained by replacing W_{mn} in the expression for c by $\bar{W}_{mn}$. It may be observed that each term in series (6) satisfies the out-of-plane boundary conditions given in eqns (4) and that the first series in eqn (8) will disappear for geometrically perfect flat plates. The prescribed in-plane boundary conditions require that

$$1-\cos\beta_k\cosh\beta_k = 0, \qquad \gamma_k = \frac{\cosh\beta_k-\cos\beta_k}{\sinh\beta_k-\sin\beta_k}. \tag{10}$$

Functions X_p and Y_q possess the orthogonality relations as follows:

$$\int_0^1 X_iX_j\,d\zeta = \int_0^1 Y_iY_j\,d\eta = \begin{cases}0, & i\neq j\\ 1, & i=j\end{cases}. \tag{11}$$

To evaluate the Fourier constants C_{pq} and F_{pq} in expression (8), eqns (6)–(8) are substituted into the compatibility equation, eqn (2). Multiplying the resulting equation by X_iY_j and integrating from 0 to 1 with respect to ζ and η, the following two sets of algebraic equations are obtained:

$$\begin{aligned}
&C_{ij}(\beta_i^4+b_4\lambda^4\beta_j^4)-\sum_{p,q=1}^{\infty}\sum C_{pq}(b_1\lambda K_1^{ip}L_2^{jq}-2b_2\lambda^2K_3^{ip}L_3^{jq}+b_3\lambda^3K_2^{ip}L_1^{jq})\\
&\quad=\frac{c\bar{c}\bar{W}_0\lambda^2}{\bar{A}_{22}}\sum\sum\sum\sum_{m,n,r,s=1,3}W_{mn}\bar{W}_{rs}(2K_4^{imr}L_4^{jns}-K_5^{imr}L_5^{jsn}-K_5^{irm}L_5^{jns})\\
&\qquad-(c\lambda^2K_R/\bar{A}_{22})\sum\sum_{m,n=1,3}W_{mn}K_6^{im}L_7^{jn}\quad i,j=1,2,3\ldots
\end{aligned} \tag{12}$$

$$\begin{aligned}
&F_{ij}(\beta_i^4+b_4\lambda^4\beta_j^4)-\sum_{p,q=1}^{\infty}\sum F_{pq}(b_1\lambda K_1^{ip}L_2^{jq}-2b_2\lambda^2K_3^{ip}L_3^{jq}+b_3\lambda^3K_2^{ip}L_1^{jq})\\
&\qquad=\frac{c^2\lambda^2}{\bar{A}_{22}}\sum\sum\sum\sum_{m,n,r,s=1,3}W_{mn}W_{rs}(K_4^{imr}L_4^{jns}-K_5^{imr}L_5^{jsn})\quad i,j=1,2,3\ldots
\end{aligned} \tag{13}$$

in which Ks and Ls are definite integrals given in the Appendix. Fourier constants in eqn (8) are thus determined from these two sets of equations.

The trail function (6) for W, the initial imperfection function (7) for $\bar{W}$ and series (8) for F satisfy the required boundary conditions (4) and compatibility equation (2) if coefficients β_p and γ_p and Fourier constants C_{pq} and F_{pq} are determined from eqns (10), (12) and (13), respectively. With these expressions, however, eqn (1) generally cannot be fulfilled.

As an approximation the Galerkin procedure is employed to furnish the following equation for the time function:

$$f_{,\tau\tau}+(\delta_1-\delta_2 n_\zeta)f+\varepsilon_1 f^2+\varepsilon_2 f^3=\delta_3 n_\zeta \tag{14}$$

where

$$\begin{aligned}\delta_1 = J\sum_{i,j,m,n=1,3}\sum\sum\sum W_{ij}W_{mn}(&K_8^{im}L_9^{jn}+a_1\lambda K_{10}^{im}L_{11}^{jn}\\&+2a_2\lambda^2 K_{12}^{im}L_{12}^{jn}+a_3\lambda^3 K_{11}^{im}L_{10}^{jn}+a_4\lambda^4 K_9^{im}L_8^{jn})\\&-\frac{J\lambda^2}{c\bar{D}_{11}}\sum_{i,j=1,3}\sum\sum\sum_{p,q=1}^{\infty}W_{ij}C_{pq}\Big[K_R K_{13}^{ip}L_7^{qj}\\&+\bar{c}\bar{W}_0\sum_{m,n=1,3}\sum\bar{W}_{mn}(K_{14}^{imp}L_5^{qjn}+K_5^{pim}L_{14}^{jnq}-2K_{15}^{imp}L_{15}^{jnq})\Big]\end{aligned} \tag{15}$$

$$\delta_2=\frac{J\lambda^2}{\bar{D}_{11}}\sum_{i,j,m,n=1,3}\sum\sum\sum W_{ij}W_{mn}(\lambda^2 r K_9^{im}L_{12}^{jn}+K_{12}^{im}L_9^{jn}) \tag{16}$$

$$\begin{aligned}\varepsilon_1 = -\frac{J\lambda^2}{c\bar{D}_{11}}\sum_{i,j=1,3}\sum\sum\sum_{p,q=1}^{\infty}W_{ij}\Big[&K_R F_{pq}K_{13}^{ip}L_7^{qj}\\&+\sum_{m,n=1,3}\sum(cW_{mn}C_{pq}+\bar{c}\bar{W}_0\bar{W}_{mn}F_{pq})(K_{14}^{imp}L_5^{qjn}+K_5^{pim}L_{14}^{jnq}-2K_{15}^{imp}L_{15}^{jnq})\Big]\end{aligned} \tag{17}$$

$$\varepsilon_2=\frac{J\lambda^2}{\bar{D}_{11}}\sum_{i,j,m,n=1,3}\sum\sum\sum\sum_{p,q=1}^{\infty}W_{ij}W_{mn}F_{pq}(2K_{15}^{imp}L_{15}^{jnq}-K_{14}^{imp}L_5^{qjn}-K_5^{pim}L_{14}^{jnq}) \tag{18}$$

$$\delta_3=\frac{J\lambda^4}{C\bar{D}_{11}}\sum_{i,j=1,3}\sum W_{ij}\Big[rK_R K_{16}^{i}L_{16}^{j}+\bar{c}\bar{W}_0\sum_{m,n=1,3}\sum\bar{W}_{mn}(rK_9^{im}L_{12}^{jn}+K_{12}^{im}L_9^{jn}/\lambda^2)\Big] \tag{19}$$

$$J=\left(\frac{\lambda^4}{\bar{D}_{11}}\sum_{i,j,m,n=1,3}\sum\sum\sum W_{ij}W_{mn}K_9^{im}L_9^{jn}\right)^{-1}. \tag{20}$$

In these equations Ks and Ls are definite integrals presented in the Appendix.

If the linear frequency is denoted by $\omega^{(0)}$, the non-dimensional linear frequency, denoted by ω_0, is related to $\omega^{(0)}$ by

$$\omega_0=\omega^{(0)}b^2/(\rho/A_{22}h^2)^{1/2}=(\delta_1-\delta_2 n_\zeta)^{1/2}. \tag{21}$$

In the case when $n_\zeta=0$ or $r=\bar{W}_0=0$ the relationship between the non-linear frequency ω and the amplitude or the maximum deflection $w_{\max}$ is, by virtue of the perturbation technique

$$\omega/\omega^{(0)}=[1+(3\varepsilon_2/4\omega_0^2-5\varepsilon_1/6\omega_0^4)W_{\max}^2]^{1/2} \tag{22}$$

where $W_{\max}$ is the ratio of $w_{\max}$ to panel thickness h.

In the postbuckling case eqn (14) reduces to

$$n_\zeta=\frac{\delta_1 W_{\max}+\varepsilon_1 W_{\max}^2+\varepsilon_2 W_{\max}^3}{\delta_3+\delta_2 W_{\max}}. \tag{23}$$

When $r=\bar{W}_0=0$, this equation is simplified to yield

Table 1. Numerical values of elastic constants

Material	E_L/E_T	G_{LT}/E_T	ν_{LT}
Glass epoxy	3	0.6	0.25
Boron–epoxy	10	1/3	0.22
Graphite–epoxy	40	0.5	0.25
Isotropic	1	0.377	0.316

Table 2. Comparison of fundamental linear frequency parameters

	$\omega^{(0)}a^2\sqrt{(\rho/D)}$ for values of a/b of						
Reference	1/3	0.4	0.5	2/3	1.0	1.5	2.5
Present	16.92	17.45	18.46	20.81	28.30	46.81	109.0
[8]	16.72	17.22	18.16	20.39	27.10	—	—
[9]	—	16.85	—	19.95	27.06	44.89	105.3

$$n_\zeta = n_{cr} + (W_{max}/\delta_2)(\varepsilon_1 + \varepsilon_2 W_{max}) \tag{24}$$

where

$$n_{cr} = (b^2/A_{22}h^2)N_{cr} = \delta_1/\delta_2 \tag{25}$$

is the non-dimensional critical buckling load with N_{cr} being the critical buckling load per unit length in the x-direction. Thus no buckling phenomenon of a cylindrical panel will occur if either the initial imperfection or the in-plane edge force in the y-direction appears.

NUMERICAL RESULTS AND DISCUSSIONS

Numerical calculations for non-linear vibration and postbuckling of shallow cylindrical panels were performed by Cyber 175 for isotropic, orthotropic and symmetrically laminated composite materials with two adjacent edges loosely clamped (C) and the other edges simply supported (SS). The laminated panel under consideration consists of an odd number of thin orthotropic plies all of the same thickness. Elastic constants typical of glass–epoxy (GL), boron–epoxy (BO) and graphite–epoxy (GR) materials are given in Table 1, where E_L and E_T are principal moduli of elasticity of an orthotropic material, G_{LT} is the shear modulus, and ν_{LT} is Poisson's ratio. In computation the constant A_{22} in eqns (3), (5), (21) and (25) is replaced by $E_T h$ without affecting the form of the other equations. In eqn (6) we take $W_{11} = 1$ and $W_{13} = 0.01$ and all other $W_{mn} = 0$. The first 16 terms in each truncated series in eqn (8) for the stress function are taken into account. The present choice of W_{ij} results in the fundamental mode of deformation and the maximum deflection is found to occur nearly at the point, $\zeta = \eta = 0.6$. In addition, the in-plane force n_y is assumed to vanish in the arc direction.

The present results for fundamental linear frequencies of an isotropic flat plate ($K_R = 0$) having different aspect ratios are compared in Table 2 with available data[8, 9]. In the table D represents the flexural rigidity of the plate. The maximum difference between the corresponding set of values is 4.6%. New results are presented graphically in the following.

In the presentation of numerical results for non-linear free flexural vibration the ratio of the fundamental non-linear frequency ω to the corresponding fundamental linear frequency $\omega^{(0)}$ is used in the plots. Thus the values of the fundamental linear frequency parameter ω_0 are presented in Table 3 such that the fundamental non-linear frequencies shown in Figs 2 and 3 can be evaluated. In the table, symmetrically laminated cross-ply cylindrical panels are represented by CP. The amplitude–frequency response curves for

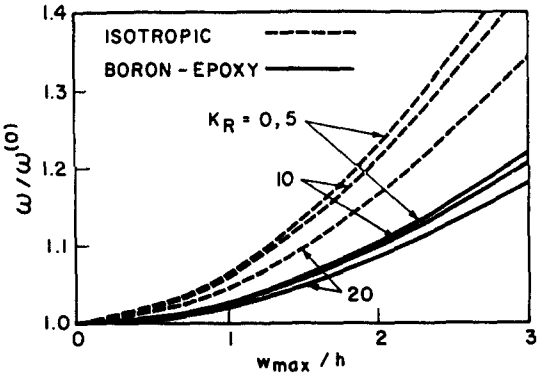

Fig. 2. Effect of the panel curvature on the fundamental non-linear frequencies of perfect isotropic and boron–epoxy orthotropic cylindrical panels ($a/b = 1$, $n_\zeta = 0$).

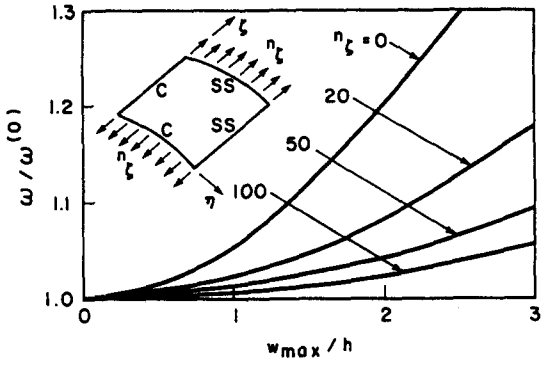

Fig. 3. Effect of uniaxial tension on the fundamental non-linear frequency of a perfect five-layer cross-ply glass–epoxy cylindrical panel ($a/b = 1$, $K_R = 15$).

Table 3. Linear frequency parameters ω_0 for cylindrical panels

Fig. 2			Fig. 3	
K_R	Isotropic	BO	n_ζ	CP
0	8.665	15.88	0	12.56
5	8.769	15.97	20	20.11
10	9.175	16.25	50	27.83
20	10.565	17.30	100	37.30

isotropic and orthotropic cylindrical panels are shown in Fig. 2 for various values of the non-dimensional curvature K_R. The result for $K_R = 0$ is the one for a flat plate. The linear and non-linear frequencies of these panels both increase with an increase in the curvature. The non-linear frequency of an orthotropic boron–epoxy panel obtained from Fig. 2 and Table 3 is roughly two times greater than that of the corresponding isotropic panel for $K_R \leqslant 20$ although the frequency ratio, $\omega/\omega^{(0)}$, is higher for the latter than for the former. It may be observed that the result for the boron–epoxy flat plate ($K_R = 0$) is approximately close to the average of the corresponding non-linear (or linear) frequencies for all-simply supported and all-clamped edges[10] in the range of the values of the amplitude considered. Figure 3 illustrates the dynamic behaviour of a symmetric cross-ply cylindrical panel composed of five layers of equal thickness for various in-plane forces in the direction of straight edges. Both linear and non-linear frequencies of the panel increase with the in-plane force although the frequency ratio does not behave so.

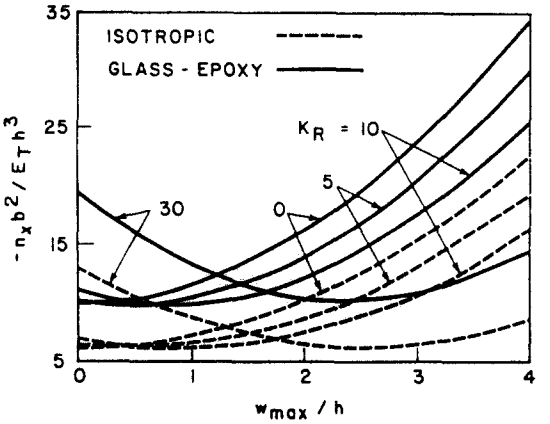

Fig. 4. Postbuckling load–deflection curves for perfect isotropic and graphite–epoxy orthotropic cylindrical panels of different curvatures ($a/b = 1$).

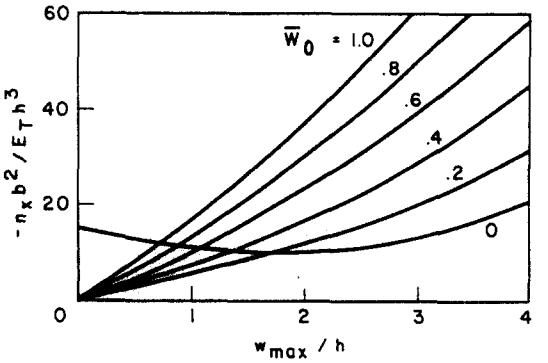

Fig. 5. Postbuckling load–deflection curves for a three-layer cross-ply glass–epoxy cylindrical panel of different initial imperfections ($a/b = 1$, $K_R = 20$, $\bar{W}_{mn} = 0$ for $m, n > 1$).

The relationship between the postbuckling load and the maximum deflection is shown in Figs 4 and 5 for cylindrical panels. Figure 4 illustrates the effect of the curvature on the postbuckling behaviour of isotropic and orthotropic cylindrical panels under uniaxial compression in the direction of straight edges. The values of $(-n_x)$ at $w_{max} = 0$ are the critical buckling loads. The maximum deflection of a flat plate ($K_R = 0$) increases with the postbuckling load in the range of the values, $w_{max}/h \leqslant 4$. The postbuckling load-carrying capacity of a cylindrical panel, however, firstly decreases and then increases with the deflection. This decrease in the load-carrying capacity is considerably significant for panels with curvatures, $K_R > 15$. The result for isotropic and glass–epoxy flat plates is, respectively, close to 89 and 91% of the average of the corresponding postbuckling loads (or critical loads) for all-simply supported and all-loosely clamped edges[11–13]. This percentage decreases slightly with increasing the postbuckling load in the range of values, $w_{max} \leqslant 4$. The effect of the initial deflection on the postbuckling load–deflection response of a laminated cross-ply cylindrical panel composed of three layers of equal thickness is shown in Fig. 5. The first term in eqn (7) for the initial deflection is taken into account. The amplitude of the initial deflection, $\bar{W}_0 = 1$, is equal to the panel thickness. The result for $\bar{W}_0 = 0$ corresponds to that for a perfect cylindrical panel. As in the case of initially deflected plates no buckling phenomenon occurs for a cylindrical panel of geometrically initial imperfections. This is because a constant term δ_3 appears in the denominator of eqn (23). Evidently a large value of $\bar{W}_0$ requires a large load for a given deflection of the panel.

CONCLUSIONS

By the use of dynamic Marguerre-type equations a single-mode analysis is carried out for symmetrically laminated cross-ply shallow cylindrical panels of geometrically initial imperfections having two adjacent edges simply supported and the other edges clamped.

The corresponding postbuckling problem is treated as a special case. Based on the present analysis some concluding remarks may be drawn.

The fundamental linear and non-linear frequencies of homogeneous and laminated cylindrical panels increase as the curvature or the in-plane edge tension increases. The present result for an orthotropic boron–epoxy flat plate is approximately close to the average of the corresponding non-linear frequencies for all-simply supported and all-loosely clamped edges.

The postbuckling load-carrying capacity of perfect homogeneous and laminated cylindrical panels firstly decreases and then increases with the maximum deflection. This decrease in the load-carrying capacity is significant for $b^2/Rh > 10$, especially for large curvatures. As in the case of flat plates no buckling phenomenon occurs for a cylindrical panel of geometrically initial imperfections. For a given deflection of a cross-ply cylindrical panel a large postbuckling load is required for a large initial deflection. The present result for isotropic and orthotropic glass–epoxy flat plates is, respectively, close to 89 and 91% of the average of the corresponding postbuckling loads for all-simply supported and all-loosely clamped edges.

Acknowledgement—The results presented in this paper were obtained in the course of research sponsored by the Natural Science and Engineering Research Council of Canada.

REFERENCES

1. C. Y. Chia, *Nonlinear Analysis of Plates*. McGraw-Hill, New York (1980).
2. J. Ramachandran, Large amplitude natural frequencies of rectangular plates with mixed boundary conditions. *J. Sound Vibr.* **45**, 295–297 (1976).
3. C. Y. Chia, Effect of boundary conditions on post-buckling of orthotropic rectangular plates. In *Instability and Plastic Collapse of Steel Structures* (Edited by L. J. Morris), pp. 303–310. Granada, London (1983).
4. C. Jiang and C. Y. Chia, Nonlinear bending of rectangular orthotropic plates with two free edges and the other edges having nonuniform rotational flexibility. *Int. J. Solids Structures* **20**, 1009–1019 (1984).
5. C. Y. Chia, Non-linear vibration of anisotropic rectangular plates with nonuniform edge constraints. *J. Sound Vibr.* **101**, 539–550 (1985).
6. C. Y. Chia, Large deflection of unsymmetric laminates with mixed boundary conditions. *Int. J. Non-Linear Mech.* **20**, 273–282 (1985).
7. C. Y. Chia, Nonlinear oscillation of unsymmetric angle-ply plate on elastic foundation having nonuniform edge supports. *Composite Struct.* **4**, 161–178 (1985).
8. T. Kanazawa and T. Kawai, On the lateral vibration on anisotropic rectangular plates. *Proc. 2nd Jap. Natl Cong. Appl. Mech.*, pp. 333–338 (1952).
9. A. W. Leissa, The free vibration of rectangular plates. *J. Sound Vibr.* **31**, 257–293 (1973).
10. M. K. Prabhakara and C. Y. Chia, Non-linear flexural vibrations of orthotropic rectangular plates. *J. Sound Vibr.* **52**, 511–518 (1977).
11. N. Yamaki, Postbuckling behaviour of rectangular plates with small initial curvature loaded in edge compression. *ASME J. Appl. Mech.* **26**, 407–414 (1959) and **27**, 335–342 (1960).
12. M. K. Prabhakara and C. Y. Chia, Post-buckling behaviour of rectangular orthotropic plates. *J. Mech. Engng Sci.* **15**, 25–33 (1973).
13. C. Y. Chia and M. K. Prabhakara, Nonlinear analysis of orthotropic plates. *J. Mech. Engng Sci.* **17**, 133–138 (1975).

APPENDIX

Constants Ks and Ls in eqns (12), (13) and (15)–(20) are given by

$$K_1^{ip} = \int_0^1 X_i X_p''' \, d\zeta \qquad K_2^{ip} = \int_0^1 X_i X_p' \, d\zeta$$

$$K_3^{ip} = \int_0^1 X_i X_p'' \, d\zeta \qquad K_4^{imr} = \int_0^1 X_i \phi_m' \phi_r' \, d\zeta$$

$$K_5^{imr} = \int_0^1 X_i \phi_m \phi_r'' \, d\zeta \qquad K_6^{im} = \int_0^1 X_i \phi_m'' \, d\zeta$$

$$L_7^{jn} = \int_0^1 Y_j \psi_n \, d\eta \qquad K_8^{im} = \int_0^1 \phi_i \phi_m^{(IV)} \, d\zeta$$

$$K_9^{im} = \int_0^1 \phi_i \phi_m \, d\zeta \qquad K_{10}^{im} = \int_0^1 \phi_i \phi_m''' \, d\zeta$$

$$K_{11}^{im} = \int_0^1 \phi_i \phi_m' \, d\zeta \qquad K_{12}^{im} = \int_0^1 \phi_i \phi_m'' \, d\zeta$$

$$K_{13}^{ip} = \int_0^1 \phi_i X_p'' \, d\zeta \qquad K_{14}^{imp} = \int_0^1 \phi_i \phi_m X_p'' \, d\zeta$$

$$K_{15}^{imp} = \int_0^1 \phi_i \phi_m' X_p' \, d\zeta \qquad K_{16}^{i} = \int_0^1 \phi_i \, d\zeta$$

and the other Ls are obtained by replacing K, i, m, p, r and ζ in the above corresponding expressions for Ks by L, j, n, q, s and η, respectively. In these expressions primes denote differentiation with respect to the corresponding coordinate.